The Perseus arm in the anticenter direction

Maria Monguió[1], Preben Grosbøl[2], and Francesca Figueras[3]

[1] Departamento de Física, Ingeniería de Sistemas y Teoría de la Señal. Escuela Politécnica Superior, Universidad de Alicante, Apdo. 99, 03080 Alicante, Spain
[2] European Southern Observatory, Karl-Schwarzschild-Str. 2, D-85748 Garching, Germany
[3] Departament d'Astronomia i Meteorologia and IEEC-ICC-UB, Universitat de Barcelona, Martí i Franquès, 1, E-08028 Barcelona, Spain

Abstract

The stellar overdensity due to the Perseus arm has been detected in the anticenter direction through individual field stars. For that purpose, a Strömgren photometric survey covering $16^{\circ2}$ was developed with the Wide Field Camera at the Isaac Newton Telescope. This photometry allowed us to compute individual physical parameters for these stars using a new method based on atmospheric models and evolutionary tracks. The analysis of the surface density as a function of distance for intermediate young stars in this survey allowed us to detect an overdensity at 1.6±0.2 kpc from the Sun, that can be associated with the Perseus arm, with a surface density amplitude of ∼14%. The significance of the detection is above 4σ for all the cases. The fit for the radial scale length of the Galactic disk provided values in the range [2.9,3.5] kpc for the population of the B4-A1 stars. We also analyzed the interstellar visual absorption distribution, and its variation as a function of distance is coherent with a dust layer before the Perseus arm location.

1   Introduction

Although it is well accepted that the Milky Way is a spiral arm Galaxy, and that these features are important agents for the dynamical evolution of the disk, there are still many open questions related with their formation, nature, and current structure. Our place inside the Galactic disk makes it a unique laboratory to study the Galaxy, but at the same time prevents us of having a complete picture of the Milky Way.

This project aims to analyze the Perseus spiral arm in the anticenter direction. Other authors have studied it considering different tracers such as HI neutral gas [7], large-scale CO distribution surveys [3], star forming complexes [14, 4], open clusters [16], or VLBI masers [11]. Most of these studies trace the arm in the second and the third quadrants, but there are very few analysis linking both, that is, pointing towards $\ell \sim 180°$.

The current project traces for the first time the arm perturbation through individual field stars. First, we show here the radial stellar density variation toward the anticenter direction by using simple star counts, and as a future work, plan to derive the distribution of the radial velocity components through this direction. To do that, we use intermediate young stars, with effective temperatures in the range [15000,9000] K (~B4-A1 spectral types). These stars are excellent tracers of this overdensity as 1) they are bright enough to reach large distances from the Sun, and 2) they are old enough so they have had time to respond to the spiral arm potential perturbation, so they are not tracing current star formation. Furthermore, to analyze the interaction between the arm and the stellar component, these stellar tracers are young enough so their intrinsic velocity is still small, so that their response to a perturbation would be stronger and therefore easier to detect.

The Strömgren photometric data and the stellar physical parameters developed for this purpose allows also to create a 3D extinction map. The analysis of the absorption distribution supports the presence of the arm perturbation and infers extra information about the nature of the spiral arm.

2 Catalog and working samples

A Strömgren photometric catalog was developed with the Wide Field Camera at the Isaac Newton Telescope covering $16^{\circ 2}$ in the anticenter direction up to $V \sim 17^m$ (see all the details in [9]). Complete $uvbyH\beta$ photometry was obtained for 35974 stars, with partial data for up to 96980 stars, all available through CDS. To compute the stellar physical parameters (SPP) for these stars we developed a new method based on atmospheric models and evolutionary tracks that provides M_V, A_V, $(b-y)_0$, T_{eff}, $\log g$ among other SPP for stars with $T_{eff} > 7000$ K. The results were compared with Hipparcos parallaxes and the errors were computed through Monte Carlo simulations. All the details were published in [10] and the catalog is also available at the CDS.

The resulting catalog of stars with physical parameters was cleaned and organized in different working samples by carefully evaluating both the quality of the data and the apparent magnitude and distance completeness. The selection of $T_{eff} > 7000$K stars, rejection of emission line stars using IPHAS data [5], rejection of outliers using different quality flags, and comparison with 2MASS data allowed us to create the three working samples MB-S1, MB-S2, and CS-MB, the first one containing more stars, but less accurate data, and the last one with very accurate data but less statistics.

Since we wanted to derive the stellar density variation as a function of the galactocentric distance, we needed to ensure that the features observed are due to a physical and real causes and not to observational or selection biases. To account for that, we created distance complete samples by selecting ranges of absolute magnitude, that ensured us distance completeness up to a given heliocentric distance. Taking into account the limiting magnitude, the magnitude at which some stars where saturated, and the absorption at each distance, we computed the minimum and maximum absolute magnitudes for each sample, in order to ensure that they are complete between 1.2 and 3 kpc. These distances were selected to have a good range before

and after the peak. The final stars selected for each sample are those with $-0.9 < M_V < 1.2$ for MB-S1 and MB-S2, and $-0.9 < M_V < 0.8$ for CS-MB.

3   The Perseus arm overdensity

To analyze the stellar disk distribution we chose the surface density over volume density since it gives an estimate of the total disk mass at a given distance. For the vertical density distribution we assumed $sech^2(z/h_z)$ [15], with h_z being the scale height of the disk. As known, h_z depends on the age of the population, so here, as an approximation, we modeled it as depending on the visual absolute magnitude of the star: $h_z(pc) = 36.8 \cdot M_V + 130.9$. It has to be taken into account that a different relation between the scale height and the intrinsic brightness would change the zero point of the stellar density distribution, and thus the corresponding surface density at the Sun position $\Sigma_\odot$. We also took into account the change in the mid-plane due to the warp modeling it as $z_W = r \cdot \tan b_W$ with $b_W \sim$-0.5° at $l = 180°$ [8].

In order to fix the zero point of the stellar density distribution, we used the catalog of Strömgren photometry [6] to compute the surface density at the Sun position for young stars. This process was done following the same methodology as we did for the anticenter stars, that is, the same computation of SPP, the same process to clean the samples, and the same M_V selection range of the stars. Then the surface density was computed assuming the same vertical density distribution. The resulting surface density vs. absolute magnitude distribution turned out to be very similar at the one obtained from a Besançon Galaxy simulation [2], with $(3.25\pm0.13)\cdot10^{-2}$ for MB-S1 and MB-S2, and $(1.70\pm0.07)\cdot10^{-2}$ for CS-MB.

We used the computed zero point to plot the surface density as a function of distance, and fit an exponential disk density function. That allowed us to recognize the overdensity associated to the Perseus arm at around 1.6 ± 0.2 kpc (slightly depending on the sample), within the distance range at which the samples are complete, that is, between 1.2 and 3 kpc from the Sun. An error of 0.2 kpc, the bin width, has been adopted for the location of the maximum overdensity. Then, we re-computed the exponential fitting avoiding the points close to the peak detected, that is between 1.4 and 2.0 kpc. In this fit, the obtained radial scale lengths are $h_R =2.9\pm0.1/0.2$ kpc for both MB-S1 and MB-S2 samples. For the cleanest sample CS-MB we obtain a slightly larger value of $h_R =3.5\pm0.5$ kpc (see Fig. 1-left). In this case, the uncertainty is significantly larger since the working sample contains less stars. In addition, the stars in this sample have a brighter apparent limiting magnitude respect to the previous ones, so their corresponding M_V range is shifted to intrinsically brighter objects, i.e., it contains a slightly younger population in mean. This result is coherent with recent data obtained from simulations [1], showing that the radial scale length is increasing when the population considered is younger.

We performed χ^2 tests for the different fits to quantitatively evaluate the significance of the detected Perseus arm overdensity using the observed number of stars for each bin, and comparing them with the distribution coming from the resulting exponential fit. The
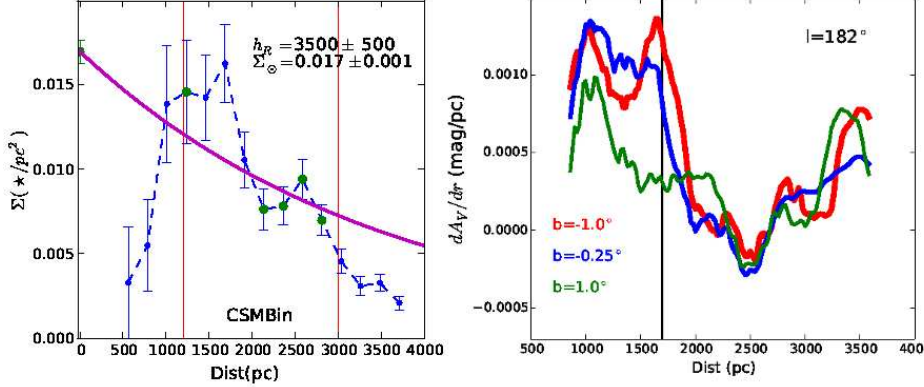
Figure 1: Left: Radial variation of the stellar surface density in blue for the CS-MB sample. Vertical red lines show the 1.2 and 3 kpc completeness limits. Green dots show the points used for the exponential fit, avoiding those around the overdensity location. The exponential fit is plotted in magenta, with the h_R and $\Sigma_\odot$ parameters expressed in pc and $\star/\mathrm{pc}^2$ respectively. Right: Differential absorption (dA_V/dr) as a function of distance for three directions.

hypothesis that the data is coming from a pure exponential distribution can be rejected at 4-5σ confidence level in all the cases. On the other hand, when we rejected the points between 1.4 and 2.0 kpc -where the overdensity is detected- and repeat the fit, we obtained p-values from the χ^2 test fully compatible with an exponential fit. We estimated the significance of the peak as $(n_{arm}^{obs} - n_{arm}^{fit})/\sqrt{n_{arm}^{obs}}$, where n_{arm}^{obs} is the number of stars in the bins close to the arm (i.e. between 1.4 and 2.0 kpc), and n_{arm}^{fit} is the expected number of stars from the exponential fit (where the arm bins were not used for the fit). The overdensity obtained for MB-S1 and MB-S2 samples had a significance of 4.3σ. For CS-MB we obtained 3.0σ, a lower value due to the smaller number of stars included in the sample. The amplitude of the arm was estimated from the expression $A = (n_{arm}^{obs} - n_{arm}^{fit})/(n_{arm}^{obs} + n_{arm}^{fit})$, obtaining $A = 0.14$ for MB-S1 and MB-S2, and $A = 0.12$ for CS-MB.

4   The Perseus arm dust layer

Since both, individual photometric distances and visual interstellar absorptions (A_V) are available for a large sample of stars, a detailed 3D extinction map was created. In Fig.2 we see some (l,b) cuts to show the 2D distribution at nine different distances of the Sun. Different features are visible there. The most relevant information obtained from this map is the distribution of absorption as a function of distance. There is a clear change of tendency at around 1.6 kpc, i.e. at the same location where the stellar overdensity was found. This is better seen when we plot the derivative as a function of distance (see Fig. 1-right). We would expect, for constant absorption, a flat distribution of the dA_V/dr, while the presence of a cloud or dust layer would be translated into a bump in the dA_V/dr distribution. So the obtained distribution is fully compatible with having a dust lane in front of the Perseus
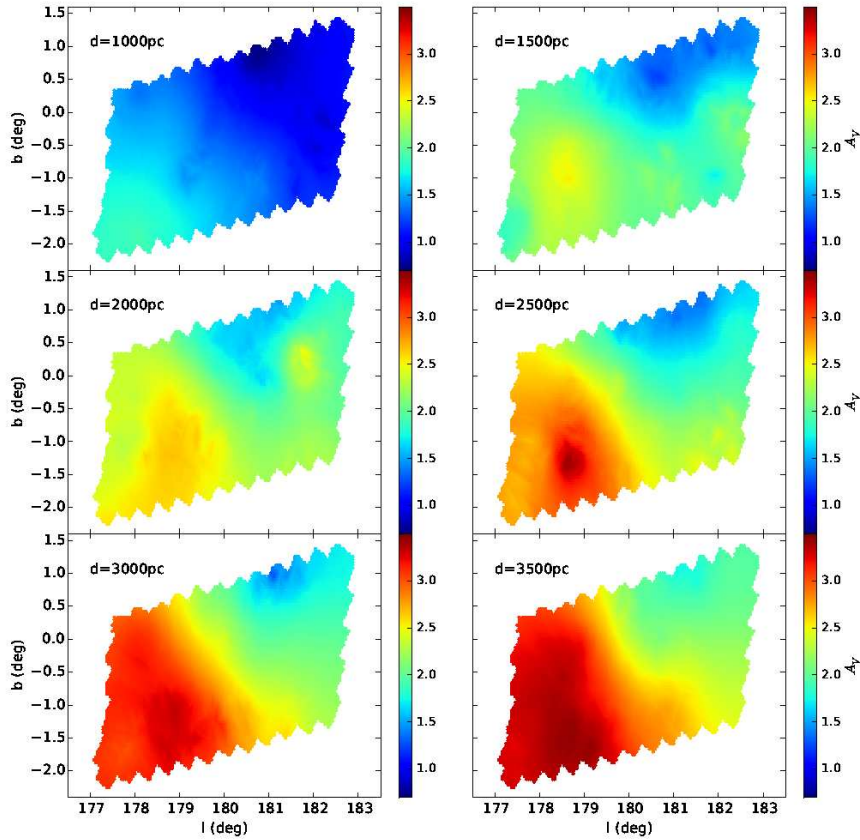
Figure 2: Cuts of the 3D extinction maps at nine different distances.

arm. The presence of the dust lane at the inner side of the stellar overdensity indicates a compression or shock in the gas associated to the spiral arm, that agrees with having it inside the corotation radius [12]. From that we can use our first analysis of the 3D extinction map to establish a limit on the corotation radius in the Milky Way Galactic disk [13]. The corotation radius of the spiral pattern (if density wave scenario is assumed) should be then outside the location of Perseus in the anticenter: $R_{CR} > 10.2\,\mathrm{kpc}$ (assuming $R_\odot = 8.5\,\mathrm{kpc}$).

5   Summary and Conclusions

In previous papers we published a deep Strömgren photometric survey, that together with a new strategy for the derivation of stellar physical parameters, allowed us to study the surface density distribution as a function of distance for the young stellar population in the anticenter direction (see [9] and [10]). Here we used these data to derive samples of intermediate young stars, complete within the distance range between 1.2 and 3.0 kpc from the Sun. We computed the surface density by assuming a vertical density distribution of the disk, taking into account the surveyed area, and the warp, so carefully defining correction functions

for all the observational and physical effects. The same strategy was used to compute the surface density at the solar neighborhood through Strömgren data [6]. The exponential functions fitted to the computed stellar surface density show a clear star overdensity at around 1.6 ± 0.2 kpc, that we associate to the presence of the Perseus spiral arm. It has been detected with a significance around 3-4σ. Our results indicate that the star density contrast of the young population in Perseus is around A=0.12-0.14. Also very important, the distribution of visual interstellar absorption as a function of distance reveals the presence of a dust layer in front of the Perseus arm, which suggests that it is placed inside the co-rotation radius of the Milky Way spiral pattern. This is the first time that the overdensity of the Perseus arm has been detected through individual star counts, and its presence is being supported by the dust distribution.

Acknowledgments

References

[1] Bird, J. C., Kazantzidis, S., Weinberg, D. H., et al. 2013, ApJ, 773, 43

[2] Czekaj, M. A., Robin, A. C., Figueras, F., Luri, X., & Haywood, M. 2014, A&A, 564, A102

[3] Dame, T. M., Hartmann, D., & Thaddeus, P. 2001, ApJ, 547, 792

[4] Foster, T. J. & Brunt, C. M. 2014, ArXiv e-prints

[5] González-Solares, E. A., Walton, N. A., Greimel, R., et al. 2008, MNRAS, 388, 89

[6] Hauck, B. & Mermilliod, M. 1998, A&AS, 129, 431

[7] Lindblad, P.O. 1967, in IAU Symposium, Vol.31, ed. H.van Woerden, 143

[8] Momany, Y., Zaggia, S., Gilmore, G., et al. 2006, A&A, 451, 515

[9] Monguió, M., Figueras, F., & Grosbøl, P. 2013, A&A, 549, A78

[10] Monguió, M., Figueras, F., & Grosbøl, P. 2014, A&A, 568, A119

[11] Reid, M. J., Menten, K. M., Brunthaler, A., et al. 2014, ApJ, 783, 130

[12] Roberts, W. W. 1969, ApJ, 158, 123

[13] Roberts, Jr., W. W. 1972, ApJ, 173, 259

[14] Russeil, D. 2003, A&A, 397, 133

[15] van der Kruit, P. C. & Searle, L. 1981, A&A, 95, 105

[16] Vázquez, R. A., May, J., Carraro, G., et al. 2008, ApJ, 672, 930